# BES Analysis Memo
# MEMO # 2: **release 0.1**
# $\chi_c$ Decays to Two Charged Hadronic Tracks

Gary S. Varner
*University of Hawaii*
varner@uhhepi.phys.hawaii.edu

February 23, 1998

**Abstract**

An analysis is performed of $\chi_{cJ}$ decays to a pair of charged hadronic tracks: $\pi^+\pi^-$, $K^+K^-$, and $p\bar{p}$. Large background from direct $\psi'$ decays, as well as non-resonant production, require removing charged leptonic final states ($e^+e^-$, $\mu^+\mu^-$) from this analysis. Because of the high momentum of the two-body final state tracks, a method of particle identification using only kinematical fitting is employed. The results of this method are compared with previous analysis using combined drift chamber $\frac{dE}{dx}$ and Time-of-Flight probability techniques. The overall efficiency of this technique is lower, but the purity of $K$ and $\pi$ samples is higher. Within errors, the branching ratio values obtained are consistent with previous BES analyses and PDG 96 values, and provide a cross-check on previous analyses.

## 1 Introduction

Utilizing the world's largest sample of resonant $\psi'$ decays, as measured by the BES collaboration during 1993-1995, a detailed study of the hadronic decay modes of the $\chi_c$ states has been undertaken. Compared with the data set for the Mark I detector[1], roughly an order of magnitude larger data set has been obtained.

Taking advantage of these larger statistics, many new modes have been observed[2][3], while others have been refined. In particular, the analysis of hadronic decay modes with small branching fractions has benefitted from larger statistics.

Reconstruction of the $\chi_c$ states in these two charged hadron modes is contaminated with background from direct $\psi'$ decays, with the predominant source of this background due to $\psi' \to \pi^0 h^+ h^-$. In these background events, one of the $\gamma$'s from the $\pi^0$ decay is mis-identified as the radiative $\gamma$ and the other $\gamma$ is lost due to acceptance, shower counter inefficiency[2] or overlap of the two $\gamma$ showers.

Due to concern about the performance of particle identification based upon combined drift chamber $\frac{dE}{dx}$ and Time-Of-Flight performance in the high momentum region populated by these high mass two-body decays, a complementary analysis has been performed. For this analysis, only kinematical fitting based on different charged particle hypotheses is made. Using simulation studies of the BES Main Drift Chamber tracking performance, which is likely the best understood component of the detector simulation, high relative efficiencies and purities for the $K$ and $\pi$ samples are obtained. The specifics of and results for this analysis are detailed below.

## 2 Event Selection

The entire BES $\psi'$ data set has been used for this analysis, which corresponds to $(3.67 \pm 0.03 \pm 0.36) \times 10^6$ produced $\psi'$s[4]. For the determination of the number of $\chi_{c_{0,1,2}}$ produced from the radiative decays of the $\psi'$s, results from the Crystal Ball detector[5] are used. This choice is dictated by the much better $\gamma$ detection efficiency and uniformity of this non-magnetic detector measurement. The values used are tabulated below:

| **Mode** | $Value \pm \sigma_{stat} \pm \sigma_{syst}$ |
|---|---|
| $\psi' \to \gamma + \chi_{c0}$ | $9.9 \pm 0.5 \pm 0.8$ % |
| $\psi' \to \gamma + \chi_{c1}$ | $9.0 \pm 0.5 \pm 0.7$ % |
| $\psi' \to \gamma + \chi_{c2}$ | $8.0 \pm 0.5 \pm 0.7$ % |

## 2.1 Fitting

A full $\psi'$ kinematic fit is performed for each event. For this task the BES standard routine *NEWSQUID* is used. Thus, for these 2 body final states, the *NEWSQUID* fit is a (4)C-fit (including the "best" $\gamma$ in the event). In this kinematical fit, for the case of events with more than one accepted photon candidate, the fits are applied for each $\gamma$ candidate and the one that gives the best fit is chosen.

For each event, this fit is performed using the five different particle hypotheses for the track pairs: $e$,$\mu$,$\pi$, K and proton. Results for the $\chi^2$ and Confidence Level of each fit species is stored for further analysis, while the particle type with the best fit is chosen to fill 4-vectors for further analysis. For accepted events, the confidence level of the best kinematic fit is required to be better than 5%.

## 2.2 General Cuts

Below are listed the general cuts used for analyzing all of the two charged track final states. In addition to the constraints mentioned briefly above, specific cuts are applied as tabulated below:

| Cut Parameter | Value | Comment |
|---|---|---|
| mfit | 2, -9, -19 | use only tracks with good fits |
| # of $\mu^{\pm}$ | $< 1$ | remove $\mu$'s using muon chamber data |
| $E_{BSC}$ | $< 0.8$ GeV | remove $e^+e^-$ via EM showers in the Barrel Shower Counter (BSC) |
| $\|cos\theta\|$ | $< 0.8$ | acceptance cut on charged, neutral particles |
| $\|cos\delta\|$ | $< 0.95$ | require $\gamma$ shower separated from charged track by approx. 18 deg |
| frmax | $< 96\%$ | require $\gamma$ shower to be spread over more than a single BSC layer |

In addition to these generic cuts, a few specific cuts are utilized to improve the signal to noise and are detailed with each mode analyzed in the next section. The choice of these specific cuts is dictated by effectiveness and efficiency in the simulation studies below.

## 2.3 $e$ and $\mu$ Contamination

Simulation of the rejection power of the general cuts above indicates that the acceptance for $e$ and $\mu$ tracks, originating from a 2-body decay in the mass region of the $\chi_{cJ}$ states, is approximately 0.2 and 0.5%, respectively. Included in these accepted events are all particle identification types. With a cut on the the opening angle, as mentioned above, contamination from Bhabha events is minimal. Therefore, the residual contamination is deemed to be small and absorbed within the conservative systematic error added to simulation results in all of these analyses[6][7].

## 2.4 $K/\pi$ Separation

As mentioned previously, concerns about the performance of the combined drift chamber $\frac{dE}{dx}$ and Time-Of-Flight for $K/\pi$ separation motivated an alternative approach. This may be seen in Figures 3.1 and 3.2 of reference [2]. With the small boost given to the $\chi_c$ state by the radiative $\gamma$ decay of the $\psi'$, the two charged hadrons should share the large momentum of this high mass decay rather equally. That is, on average, each low-mass track is expected to have a momentum around $1.5GeV$. In this regime, the particle identification performance of these techniques is dubious at best.

Utilizing the fact that $e$ and $\mu$ contamination is indicated to be small, for subsequent discussion, all particles which are identified by the fitting algorithm to be $e$, $\mu$ or $\pi$, will be assigned to be a pion pair. This is justified by the fact that fitting errors on simulated $\pi^+\pi^-$ decays are very often reconstructed slightly better as an $e^+e^-$, $\mu^+\mu^-$ pair, because of the low masses of the charged pions.

By studying the cases in simulation in which the $\pi$'s and $K$'s were misidentified, it was noticed that mis-tagging was often associated with a flat distribution of $\chi^2$ fit values across the low-mass and $K$ mass hypotheses. Interpretation of this observation is quite straightforward: misidentification is associated with a sloppy fit, which can accomodate a broad range of masses. A number of different means of parameterizing this "goodness" of fit were tried. Most of these were inspired by trying a $\chi^2$ slope parameterization among the low-mass states and between them and the K mass. In the end, the simplest and most powerful was simply the absolute difference in the $\chi^2$ of the fit between the $\pi$ and $K$ masses.

Using a Monte Carlo sample of $10^4$ decays per $\chi_c$ mode, Figures 1 and 2 show the results, respectively, for the $\pi$ and $K$ simulations. In these two figures, the upper plots, labelled (a) and (b), are for the correct Particle Identification (PID), while the lower plots show the incorrect PID.

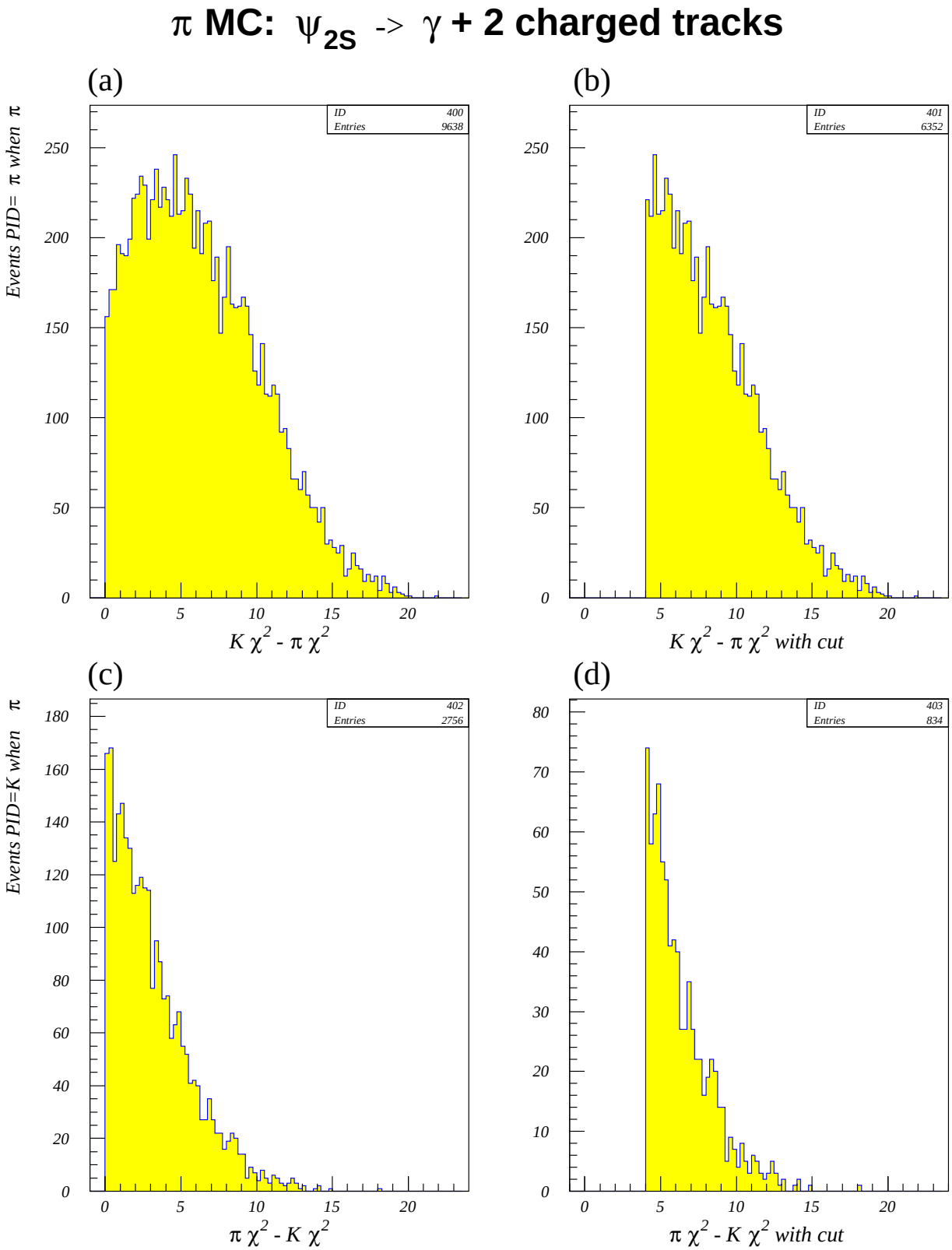


Figure 1: Plots of the results from kinematic fits to extract the particle identification (PID) of simulated $\chi_{c_J}$ decays to $\pi^+\pi^-$. On the top, (a) and (b), are the distributions of $|\chi^2(K) - \chi^2(\pi)|$ for correct PID. Plots (c) and (d) are for incorrect PID. Notice that this parameter is peaked at low value for incorrect PID assignment, a fact which is used to improve PID relative efficiency and purity. Results for the cut chosen are shown in plots (b) and (d), and summarized in the text.

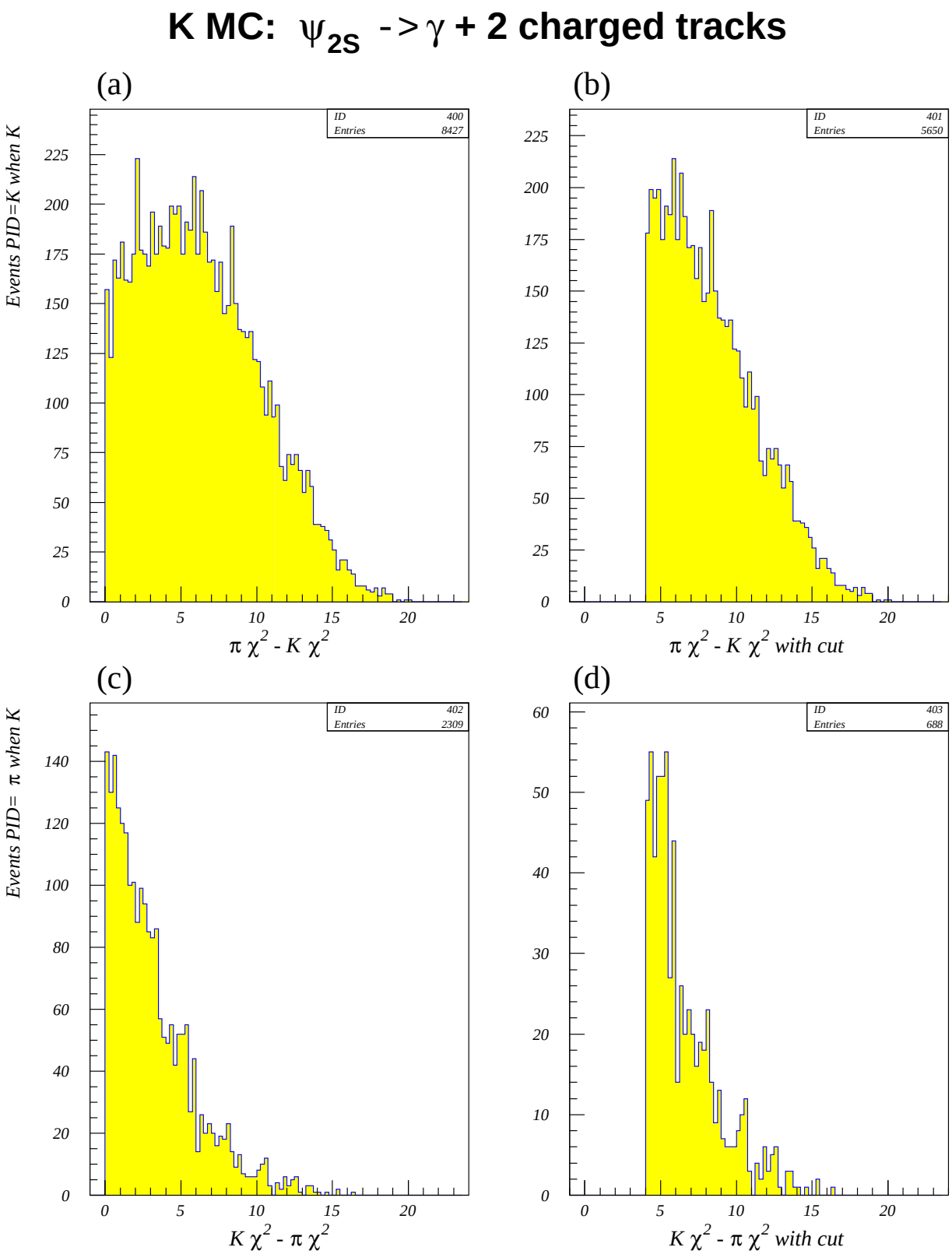


Figure 2: Plots of the results from kinematic fits to extract the particle identification (PID) of simulated $\chi_{cJ}$ decays to $K^+K^-$. On the top, (a) and (b), are the distributions of $|\chi^2(K) - \chi^2(\pi)|$ for correct PID. Plots (c) and (d) are for incorrect PID. Notice that this parameter is peaked at low value for incorrect PID assignment, a fact which is used to improve PID relative efficiency and purity. Results for the cut chosen are shown in plots (b) and (d), and summarized in the text.

On the left two plots, (a) and (c), are values without a cut applied, while (b), (d) show the distributions with the final cut value applied. As expected, in both sets of plots the wrong PID distribution is peaked at low $\chi^2$ difference. While a choice of final cut value is a matter of subjective preference, the table below summarizes the trade-offs in terms of statistics loss, PID purity and PID relative tagging efficiency. Performance versus cut value is a fairly gradual function, and thus only two of the representative points, considered as cut value candidates, are tabulated below.

**$\pi$ PID versus $|(\chi^2(K) - \chi^2(\pi)|$ Cut Value**

| Quantity | Function | Cut = 0 | Cut = 4.0 | Cut = 6.0 |
|---|---|---|---|---|
| Purity | $\frac{\pi_{real}}{\pi_{real}+\pi_{fake}}$ | 80.7% | 90.2% | 93.6% |
| Efficiency | $\frac{\pi_{real}}{\pi_{real}+K_{fake}}$ | 77.8% | 88.4% | 92.3% |
| Data Fraction | $\frac{\pi_{real}^{cut}}{\pi_{real}^{no\ cut}}$ | 100% | 65.9% | 47.7% |

**$K$ PID versus $|(\chi^2(K) - \chi^2(\pi)|$ Cut Value**

| Quantity | Function | Cut = 0 | Cut = 4.0 | Cut = 6.0 |
|---|---|---|---|---|
| Purity | $\frac{K_{real}}{K_{real}+K_{fake}}$ | 75.3% | 87.1% | 91.5% |
| Efficiency | $\frac{K_{real}}{K_{real}+\pi_{fake}}$ | 78.5% | 89.1% | 92.9% |
| Data Fraction | $\frac{K_{real}^{cut}}{K_{real}^{no\ cut}}$ | 100% | 67.0% | 48.8% |

Placing the cut at $\Delta\chi^2 > 4.0$ corresponds to PID purities and relative efficiencies of approximately 90%, while retaining about two-thirds of the original data, for both $\pi$ and $K$. Moving the cut up to 6.0 improves the purity and relative efficiency a few percent, while reducing the data set to approximately half of the original volume. On this basis, a cut value of 4.0 was chosen.

Note that the total number of original $\pi$ and $K$, before cuts, in both the data and Monte Carlo sets are roughly the same, meaning that after applying these cuts, a correction isn't needed for the relative efficiency, since the loss of efficiency is almost matched by the cross-over from mis-identification. Nevertheless, to be conservative, a systematic error of 10% has been assigned to the extracted number of events in the analysis that follows.

If these numbers are compared with the values anticipated from the combined probability method (MDC $\frac{dE}{dx}$ + TOF), this is a substantial improvement in both purity and relative efficiency, albeit with somewhat reduced statistics.

### 2.5 $p\bar{p}$ Identification

Due to their high masses, $p\bar{p}$ decays of the $\chi_c$ states are clearly distinguished kinematically from the lower mass pairs considered above. Quantitatively, simulation shows misidentification as a $K^+K^-$ pair to be about 0.1% and completely negligible for lower masses. Thus, $p\bar{p}$ PID relative efficiency is essentially 100%. The purity is more than 99%, where the dominant contaminant is $K^+K^-$ misidentification as $p\bar{p}$ at a level of about 0.5%.

As is seen in the data extraction fits below, the lack of statistics is the dominant error contribution. Therefore, no further cuts were done to improve this already quite pure particle identification sample. However, this mode remains rather seriously swamped with $\psi' \to \pi^0 p\bar{p}$ background. Attempts to improve signal to noise are discussed in the $p\bar{p}$ results section below.

### 2.6 Single Pass Assignment

To avoid problems of double counting events, the reconstructed data tapes were processed once and all subsequent analysis makes use of the kinematic fit PID flag for selecting the decay mode to process further. As mentioned above, in all cases below, PID fits to $e$ and $\mu$ are assigned to be $\pi$'s.

# 3 $\pi^+\pi^-$ Results

Utilizing only the general cuts and $|\chi^2(K) - \chi^2(\pi)| > 4.0$, the results for data and simulation are shown in Figure 3. A tabulation of the branching fraction results are displayed in Figure 4.

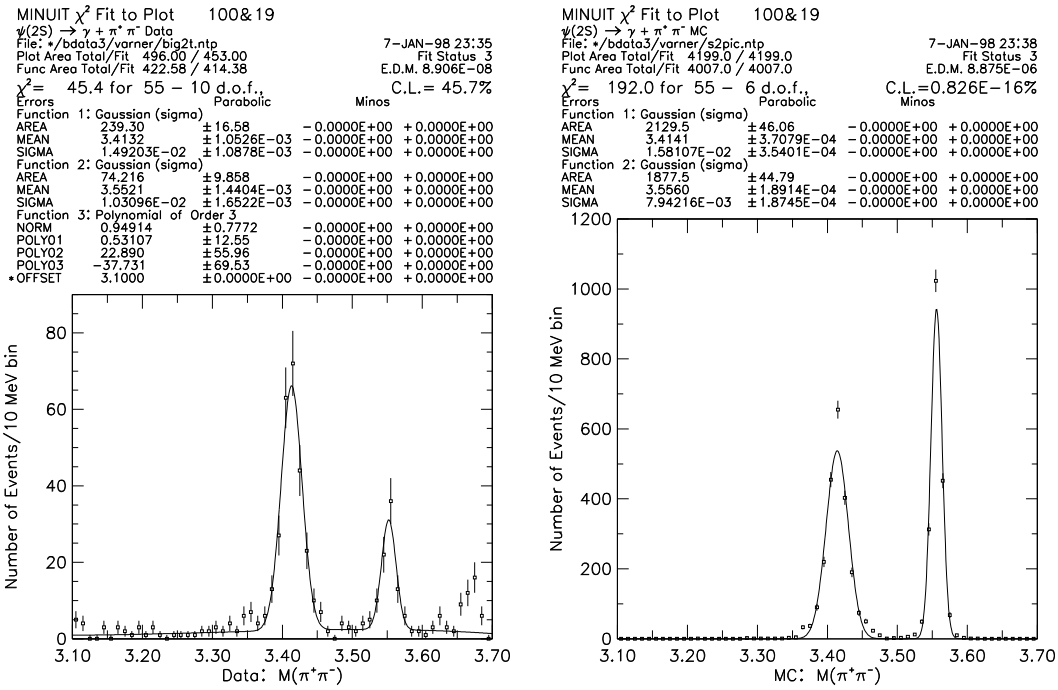


Figure 3: Reconstructed mass plots for $\chi_{cJ}$ decays to $\pi^+\pi^-$. Data shown on the left, $10^4$ simulated events per $\chi_{c0,2}$ on the right.

**π+π− Analysis**

| | | | <Value> | σ stat | σ sys | | Fit σ sys: | 10% |
|---|---|---|---|---|---|---|---|---|
| Purity: | 90.2% | | | | | | | |
| Efficiency: | 88.4% | N(ψ') | 3.67E+06 | 3.00E+04 | 3.60E+05 | | MC σ sys: | 7.8% |

| | γ+χc0 | | | γ+χc1 | | | γ+χc2 | | |
|---|---|---|---|---|---|---|---|---|---|
| B(ψ' -> X) | 9.9% | 0.5% | 0.8% | 9.0% | 0.5% | 0.7% | 8.0% | 0.5% | 0.7% |
| ηdet | 21.3% | 0.5% | 1.7% | | | | 18.8% | 0.4% | 1.5% |
| N(χc) | 363330 | 18589 | 46176 | 330300 | 18548 | 41349 | 293600 | 18506 | 38593 |
| N(χc) det | 77353 | 4297 | 11535 | | | | 55123 | 3715 | 8425 |
| Nevts | 239.3 | 16.6 | 23.9 | | | | 74.2 | 9.9 | 7.4 |
| B(X->π+π-) | 3.09 | 0.27 | 0.56 | | | | 1.35 | 0.20 | 0.25 |
| (x10^-3) | 3.1 | 0.3 | 0.6 | | | | 1.3 | 0.2 | 0.2 |
| combined Errors: | 3.1 | 0.6 | | | | | 1.3 | 0.3 | |

Figure 4: Summary table for the $\chi_{c0}, \chi_{c2}$ decays to the $\pi^+\pi^-$ final state. Note that a 10% systematic error has been added to the extracted number of events to account for final state impurity.

# 4 $K^+K^-$ Results

Utilizing only the general cuts and $|\chi^2(K) - \chi^2(\pi)| > 4.0$, the results for data and simulation are shown in Figure 5. A tabulation of the branching fraction results are displayed in Figure 6. It is interesting to compare Figures 3 and 5. Note that an obvious $\psi'$ background peak, just to the low-mass side of the $\psi'$ at $3.68GeV$, is present in the case of $\pi^+\pi^-$ and absent for $K^+K^-$. This doesn't match expectation from the relative branching ratios[8] for direct $\psi' \to K^+K^-$ with BR $= (1.0 \pm 0.7) \times 10^{-4}$ versus $\psi' \to \pi^+\pi^-$ with BR $= (8 \pm 5) \times 10^{-5}$.

However, given that this background mode requires a ficticious $\gamma$ to be reconstructed, which may have different systematics in the fitting for different decay masses, this is probably not a major concern.

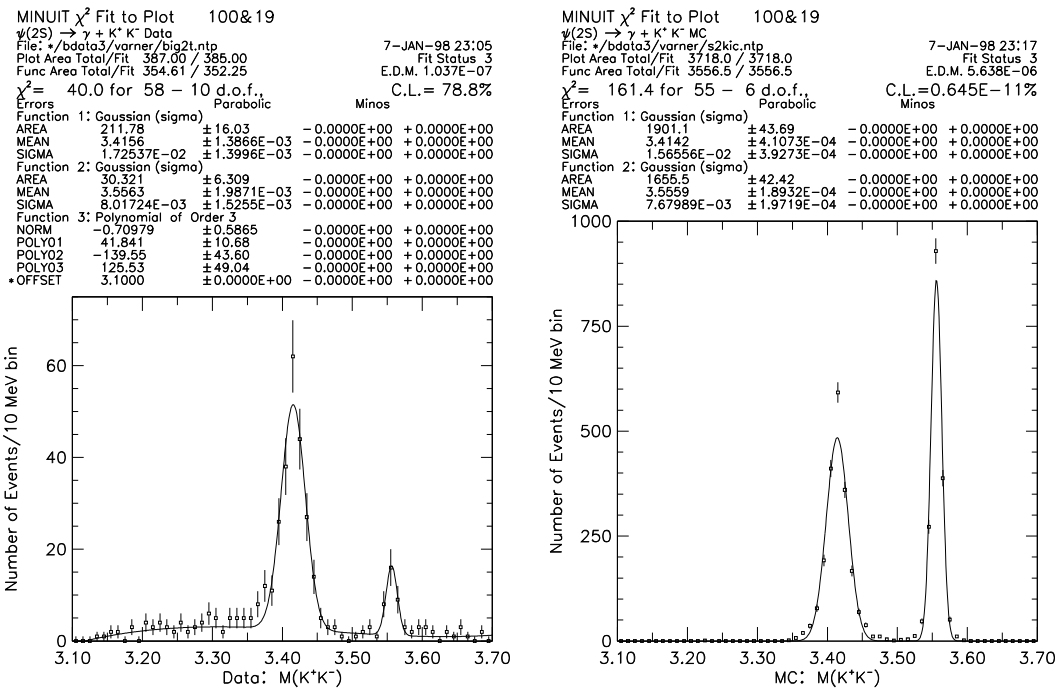


Figure 5: On the left is the fit to the data to extract the number of events, and on the right is the fit to extract the detection efficiency for $\chi_{c_J} \to K^+K^-$. There are $10^4$ simulated decays per $\chi_{c_0}$ and $\chi_{c_2}$.

K+K− **Analysis**

| | | | <Value> | σ stat | σ sys | | Fit σ sys: | 10% |
|---|---|---|---|---|---|---|---|---|
| Purity: | 87.1% | | | | | | | |
| Efficiency: | 89.1% | | N(ψ') | 3.67E+06 | 3.00E+04 | 3.60E+05 | MC σ sys: | 7.8% |

| | γ+χc0 | | | γ+χc1 | | | γ+χc2 | | |
|---|---|---|---|---|---|---|---|---|---|
| B(ψ' -> X) | 9.9% | 0.5% | 0.8% | 9.0% | 0.5% | 0.7% | 8.0% | 0.5% | 0.7% |
| ηdet | 19.0% | 0.4% | 1.5% | | | | 16.6% | 0.42% | 1.29% |
| N(χc) | 363330 | 18589 | 46176 | 330300 | 18548 | 41349 | 293600 | 18506 | 38593 |
| N(χc) det | 69033 | 3877 | 10294 | | | | 48620 | 3308 | 7431 |
| Nevts | 211.8 | 16.0 | 21.2 | | | | 30.3 | 6.3 | 3.0 |
| B(X->K+ K-) | 3.07 | 0.29 | 0.55 | | | | 0.62 | 0.14 | 0.11 |
| (x10^-3) | 3.1 | 0.3 | 0.6 | | | | 0.6 | 0.1 | 0.1 |
| combined Errors: | 3.1 | 0.6 | | | | | 0.6 | 0.2 | |

Figure 6: Summary table for $\chi_{c_{0,2}}$ decays to the $K^+K^-$ final state. Note that a 10% systematic error has been added to the extracted number of events to account for final state impurity.

# 5 $p\bar{p}$ Results

Unlike the previous two modes, this one is swamped with background, with respect to a rather weak signal. After varying numerous cuts and seeing a very large sensitivity in the signal to noise ratio, it is the author's assessment that the systematic error reported by C.Z. Yuan is seriously underestimated. In particular, the signal significance reported in reference [2] for the $\chi_{c_0}$ is not robust against slight modification to the background cuts. After considerable manipulation of parameters, the following choice of cuts were taken: $|cos\gamma| < 0.4$, # of good $\gamma$'s $= 1$ (with confidence level $> 1\%$), proton fit confidence level $> 5\%$, and $E_\gamma > 80MeV$.

Applying these cuts, the results for data and simulation are shown in Figure 7. A tabulation of the branching fraction results are displayed in Figure 8.

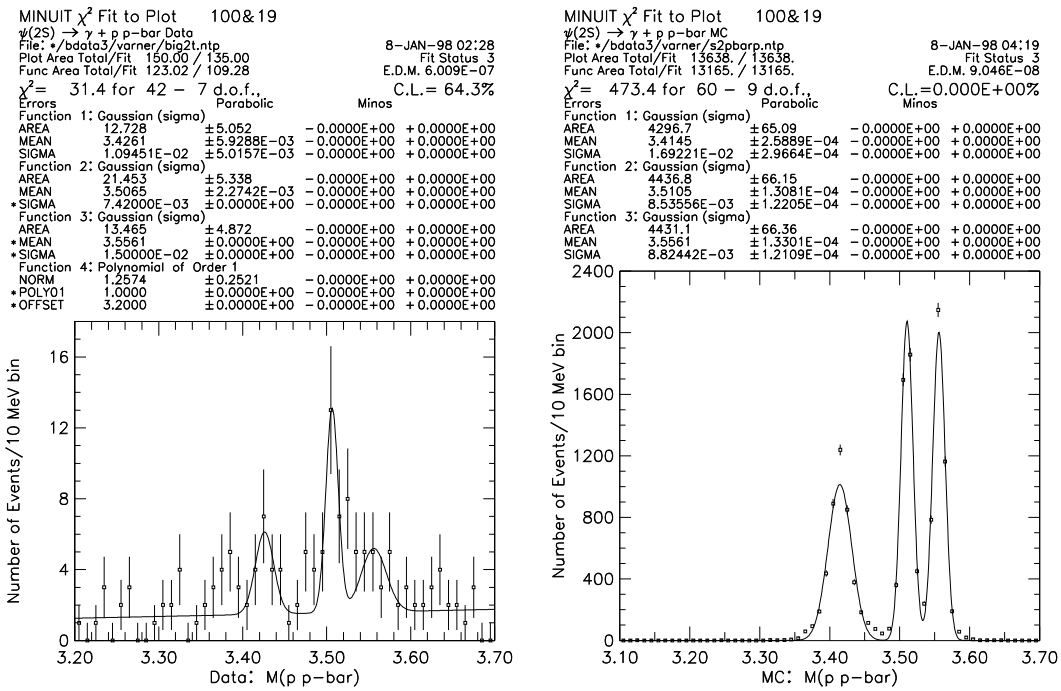


Figure 7: Measurement of $\chi_{c_J} \to p\bar{p}$. Data on the left and simulation on the right.

**p-bar p Analysis**

| | <Value> | σ stat | σ sys | | Fit σ sys: | 5% |
|---|---|---|---|---|---|---|
| N(ψ') | 3.67E+06 | 3.00E+04 | 3.60E+05 | | MC σ sys: | 7.8% |

| | γ+χc0 | | | γ+χc1 | | | γ+χc2 | | |
|---|---|---|---|---|---|---|---|---|---|
| B(ψ' -> X) | 9.9% | 0.5% | 0.8% | 9.0% | 0.5% | 0.7% | 8.0% | 0.5% | 0.7% |
| | | | | | | | | | |
| ηdet | 43.0% | 0.7% | 3.4% | 44.4% | 0.7% | 3.5% | 44.3% | 0.66% | 3.46% |
| | | | | | | | | | |
| N(χc) | 363330 | 18589 | 46176 | 330300 | 18548 | 41349 | 293600 | 18506 | 38593 |
| | | | | | | | | | |
| N(χc) det | 156112 | 8330 | 23279 | 146554 | 8513 | 21616 | 130065 | 8427 | 19880 |
| | | | | | | | | | |
| Nevts | 12.7 | 5.1 | 0.6 | 21.4 | 5.3 | 1.1 | 13.5 | 4.9 | 0.7 |
| | | | | | | | | | |
| B(X->p p-bar) | 8.14 | 3.30 | 1.28 | 14.60 | 3.71 | 2.27 | 10.38 | 3.83 | 1.67 |
| (x10^-5) | 8.1 | 3.3 | 1.3 | 14.6 | 3.7 | 2.3 | 10.4 | 3.8 | 1.7 |
| combined Errors: | 8.1 | 3.5 | | 14.6 | 4.4 | | 10.4 | 4.2 | |

Figure 8: Summary table of the decays to $\chi_{c_J} \to p\bar{p}$. Note that the $\chi_{c_0}$ signal is quite weak ($\approx 2\sigma$), while the $\chi_{c_1}$ signal is quite robust, and is far less dependent upon background cuts. This is exactly opposite to the results reported in reference[2], Figure 7.3.

# 6 Summary

The results of this analysis may be summarized as follows:

1. $\pi^+\pi^- Decays$: Relative Efficiency = 88.4%, Purity = 90.2%
   - $\chi_{c_0} \longrightarrow \pi^+\pi^-$ has BR = $(3.09 \pm 0.27 \pm 0.56) \times 10^{-3}$
   - $\chi_{c_2} \longrightarrow \pi^+\pi^-$ has BR = $(1.35 \pm 0.20 \pm 0.25) \times 10^{-3}$
2. $K^+K^- Decays$: Relative Efficiency = 89.1%, Purity = 87.1%
   - $\chi_{c_0} \longrightarrow K^+K^-$ has BR = $(3.07 \pm 0.29 \pm 0.55) \times 10^{-3}$
   - $\chi_{c_2} \longrightarrow \pi^+\pi^-$ has BR = $(0.62 \pm 0.14 \pm 0.11) \times 10^{-3}$
3. $p\bar{p}$ $Decays$: Relative Efficiency $\approx 100\%$, Purity $> 99\%$
   - $\chi_{c_0} \longrightarrow p\bar{p}$ has BR = $(8.14 \pm 3.30 \pm 1.28) \times 10^{-5}$
   - $\chi_{c_1} \longrightarrow p\bar{p}$ has BR = $(14.60 \pm 3.71 \pm 2.27) \times 10^{-5}$
   - $\chi_{c_2} \longrightarrow p\bar{p}$ has BR = $(10.38 \pm 3.83 \pm 1.67) \times 10^{-5}$

The table below shows the comparison of this analysis with those reported previously, demonstrating the consistency of these results.

| **Mode** | **# evts** | **this analysis** | **# evts** | **C.Z. Yuan** | **# evts** | **PDG 96** |
|---|---|---|---|---|---|---|
| $B(\chi_{c_0} \to \pi^+\pi^-) \times 10^{-3}$ | $239 \pm 17 \pm 24$ | $3.09 \pm 0.27 \pm 0.56$ | $350 \pm 19$ | $4.27 \pm 0.23 \pm 0.60$ | $32 \pm 6$ | $7.5 \pm 2.1$ |
| $B(\chi_{c_2} \to \pi^+\pi^-) \times 10^{-3}$ | $74 \pm 10 \pm 7$ | $1.35 \pm 0.20 \pm 0.25$ | $84 \pm 9$ | $1.52 \pm 0.17 \pm 0.29$ | 4 | $1.9 \pm 1.0$ |
| $B(\chi_{c_0} \to K^+K^-) \times 10^{-3}$ | $212 \pm 16 \pm 21$ | $3.07 \pm 0.29 \pm 0.55$ | $258 \pm 16$ | $3.44 \pm 0.21 \pm 0.47$ | $27 \pm 5.5$ | $7.1 \pm 2.4$ |
| $B(\chi_{c_2} \to K^+K^-) \times 10^{-3}$ | $30 \pm 6 \pm 3$ | $0.62 \pm 0.14 \pm 0.11$ | $24 \pm 5$ | $0.52 \pm 0.11 \pm 0.18$ | 2 | $1.5 \pm 1.1$ |
| $B(\chi_{c_0} \to p\bar{p}) \times 10^{-5}$ | $12.7 \pm 5.1$ | $8.1 \pm 3.3 \pm 1.3$ | $16.4 \pm 4.2$ | $14.4 \pm 3.7 \pm 3.1$ | | $< 90.$ |
| $B(\chi_{c_1} \to p\bar{p}) \times 10^{-5}$ | $21.4 \pm 5.4$ | $14.6 \pm 3.7 \pm 2.3$ | $6.8 \pm 3.0$ | $5.9 \pm 2.6 \pm 1.9$ | 513 | $8.6 \pm 1.2$ |
| $B(\chi_{c_2} \to p\bar{p}) \times 10^{-5}$ | $13.5 \pm 4.9$ | $10.4 \pm 3.8 \pm 1.7$ | $7.9 \pm 3.1$ | $8.6 \pm 3.4 \pm 3.7$ | 585 | $10.0 \pm 1.0$ |

# References


[1] W. Tannenbaum *et al.*, Phys. Rev. **D17**, 1731 (1978).

[2] C.Z. Yuan, *Ph.D. Thesis [in Chinese]*, 1997.

[3] G.S. Varner "Analysis Note: $\chi_{cJ}$ Decays to High Multiplicity $\pi^+\pi^-$ Pairs", BES Analysis Memo, Dec. 1997.

[4] F.A. Harris, "Analysis Note: Number of $\psi'$ Events", BES Analysis Memo, 1997.

[5] C. Edwards *et al.*, Phys. Rev. Lett. **48**, 70 (1982).

[6] G.S. Varner, *A Note on Systematic Errors*, $\psi'$ Group Internal Note, Feb. 1998.

[7] G.S. Varner, *Ph.D. Thesis*, due 1998.

[8] R.M. Barnett *et al.*, Phys. Rev. **D54**, 1 (1996).